# Worm-to-Sphere Shape Transition of Thermoresponsive Linear Molecular Bottlebrushes in Moderately Concentrated Aqueous Solution

Daniel M. Henn, <sup>‡</sup> Jessica A. Holmes, <sup>‡</sup> Ethan W. Kent, and Bin Zhao\*

Department of Chemistry, University of Tennessee, Knoxville, Tennessee 37996, United States

<sup>‡</sup> These authors contributed equally to this work.

\* Corresponding author. Email: bzhao@utk.edu (B.Z.)

#### Abstract

Molecular bottlebrushes have been shown to exhibit intriguing worm-to-sphere shape transitions in response to external stimuli. However, such shape changing has been restricted to dilute solutions, typically < 1.0 mg/g, or at interfaces. Here we report a method for achieving worm-to-sphere shape transitions of linear molecular bottlebrushes in moderately concentrated aqueous solutions by using binary heterografted molecular brushes composed of a poly(ethylene oxide) (PEO) and a thermoresponsive polymer as side chains. The PEO was designed to be significantly longer so that the thermoresponsive side chains were well shielded by PEO to avoid intermolecular association during the lower critical solution temperature transition. To facilitate the analysis by dynamic light scattering (DLS) and atomic force microscopy (AFM), a suitable amount of crosslinkable cinnamate groups was introduced into the thermoresponsive polymer, allowing fixing of the brush shape at higher temperatures by UV irradiation. To demonstrate the effect of relative chain lengths of the two side chain polymers, three brush polymers, BMB-5k, -2k, and -750, were synthesized by grafting an alkyne end-functionalized thermoresponsive, UV-crosslinkable polymer with a DP of 43 and a PEO with a DP of 114, 45, or 17, respectively, in a

molar ratio of 1:1 onto an azide-bearing backbone polymer via copper (I)-catalyzed click reaction. While BMB-2k and -750 underwent intermolecular aggregation in water at a concentration of 10 mg/g upon heating, DLS and AFM studies showed that BMB-5k collapsed intramolecularly and transformed from a wormlike to a spherical shape at concentrations of 10 and 25 mg/g. Even at a concentration of 100 mg/g, at least 95% of brush molecules underwent a worm-to-sphere transition from AFM analysis of the UV-crosslinked BMB-5k at a higher temperature. The method reported here may enable new opportunities for potential applications of shape changing molecular brushes.

#### Introduction

The biological functions of natural proteins are governed by their shapes, and it is vitally important for proteins to fold correctly in cells once synthesized. On the other hand, certain globular proteins perform their functions upon unfolding. For example, the von Willebrand factor (VWF),<sup>2,3</sup> which plays an important role in blood clotting, and Talin,<sup>4,5</sup> which is involved in cellular adhesion events, undergo unraveling from compact to stretched conformations in response to (bio)chemical or mechanical signals, exposing the buried interaction sites for subsequent binding. Molecular bottlebrushes, 6-37 which are composed of densely grafted polymeric side chains on a polymer backbone and have been shown to exhibit reversible worm-to-sphere shape transitions in response to external stimuli, 17-37 are excellent synthetic polymers for mimicking the folding and unfolding behavior of proteins. However, unlike proteins, which can fold correctly into their native conformations at a high protein concentration (e.g., 100 mg/mL) in biological cells due to the assistance of chaperone proteins or other biological macromolecules, the shape changing of stimuli-responsive molecular bottlebrushes has been restricted to rather dilute conditions, <sup>17-20,25,31</sup> typically < 1.0 mg/g, or at interfaces. <sup>21-24</sup> Higher concentrations inevitably lead to intermolecular aggregation, as often evidenced by clear-to-cloudy transitions of molecular brush solutions in response to external stimuli. This has greatly limited the use of this class of intriguing complex macromolecules in potential applications, such as delivery of substances, biomimetic catalysis, viscosity modification, etc.

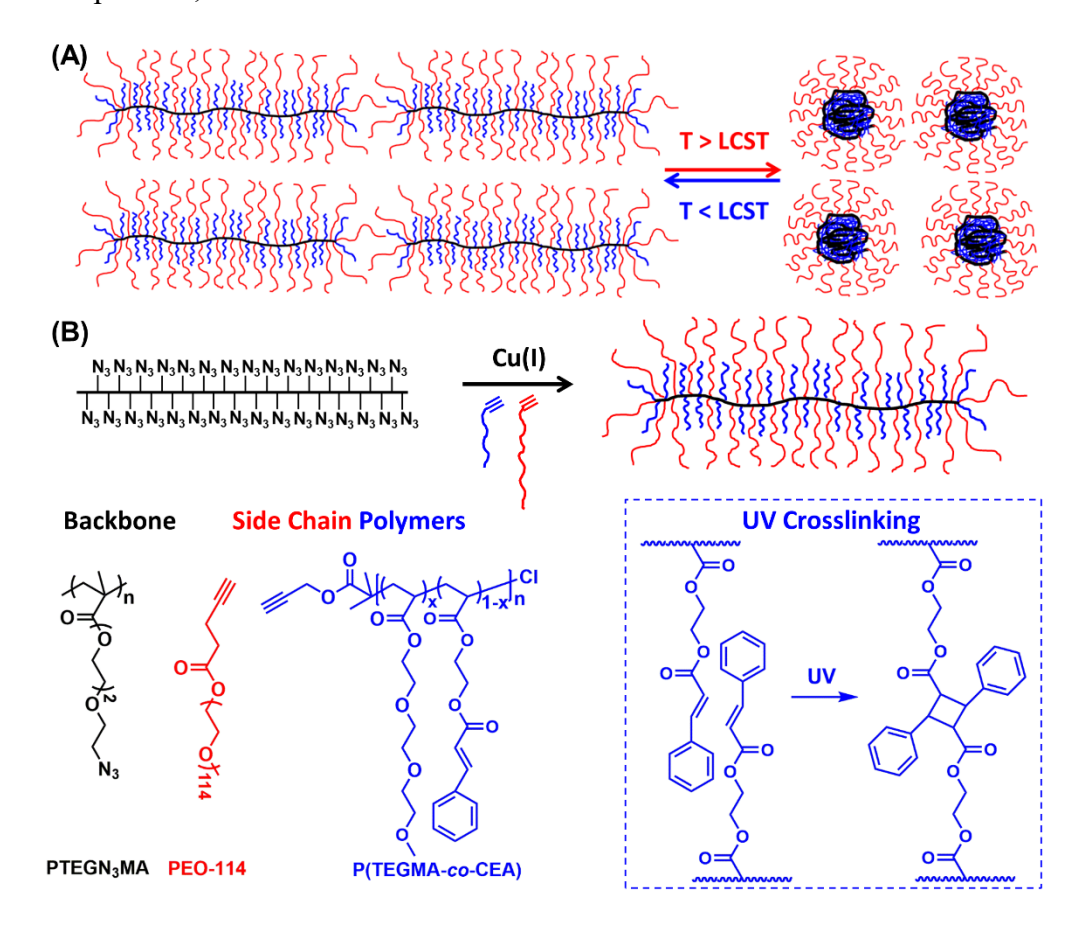
We recently reported binary heterografted linear molecular bottlebrushes composed of a poly(ethylene oxide) (PEO) and a thermoresponsive polymer as side chains.<sup>36</sup> The water-soluble PEO was introduced to stabilize the collapsed, thermoresponsive side chains at temperatures above the lower critical solution temperature (LCST). The brushes were synthesized by a "grafting to"

method using the highly efficient copper(I)-catalyzed azide-alkyne cycloaddition click reaction.<sup>36-40</sup> These thermoresponsive heterografted molecular brushes exhibited reversible shape transitions between wormlike and globular conformations in water at a concentration of 1.0 mg/g in response to temperature changes, while at the same concentration the aqueous solution of homografted thermoresponsive molecular brushes turned cloudy upon heating above the LCST.<sup>36</sup> By incorporating biotin into the thermoresponsive side chains, we showed that the thermally induced shape changing of heterografted molecular brushes can be used to control the binding interactions of biotin moieties in the brushes and avidin in the environment.<sup>36</sup>

The worm-to-sphere shape changing of molecular bottlebrushes has been thought to start from the collapse of side chains onto the backbone polymer, causing the backbone to undergo axial contraction and the brush molecules to eventually transform into a spherical shape.<sup>23</sup> Upon heating across the LCST, the longer thermoresponsive side chains in molecular bottlebrushes likely will shrink and collapse onto the backbone first, because of their slightly lower transition temperature, 41,42 followed by the collapse of short ones. Considering this scenario, we hypothesized that worm-to-sphere transitions of linear molecular bottlebrushes can be achieved in moderately concentrated solutions if the stimuli-responsive polymer side chains are well shielded from those in the neighboring brush molecules by the longer non-responsive polymer side chains (i.e., if the stabilizing side chains are much longer than stimuli-responsive side chains) (Scheme 1A). As such, the intermolecular association of stimuli-responsive side chains from different brush molecules can be effectively prevented. To explore this hypothesis, we designed and synthesized binary heterografted linear molecular bottlebrushes composed of a PEO with a molecular weight of 5,000 Da (DP = 114) and a thermoresponsive, UV-crosslinkable polymer with a DP of 43, P(TEGMA-co-CEA), as side chains (BMB-5k) (Scheme 1B). The UV-crosslinkable cinnamate

groups<sup>43,44</sup> were introduced into the thermoresponsive polymer to allow for the crosslinking of brushes in the collapsed state at a higher temperature and thus the fixation of the spherical shape for convenient characterization at lower temperatures and after dilution. We show in this work that worm-to-sphere shape changing of BMB-5k can be achieved in moderately concentrated aqueous solutions.

**Scheme 1.** (A) Worm-to-Sphere Shape Transition of Thermoresponsive Binary Heterografted Linear Molecular Bottlebrushes in Moderately Concentrated Aqueous Solutions and (B) Synthesis of Thermoresponsive, UV-Crosslinkable Molecular Bottlebrushes.



### **Experimental Section**

**Materials.** *N*,*N*,*N*',*N*'',*N*''-Pentamethyldiethylenetriamine (PMDETA, 99%, Acros) and ethyl 2-bromoisobutyrate (98%, Aldrich) were dried over calcium hydride, vacuum distilled, and stored

in dessicators. CuBr (98%, Aldrich) was stirred in glacial acetic acid overnight, filtered, and washed with absolute ethanol and diethyl ether, which was then collected, dried under vacuum, and stored in a desiccator. Copper (I) chloride (purified, 99%) and sodium azide (99%) were purchased from Acros and used as received. The azide-functionalized backbone polymer, poly(2-(2-(2-azidylethoxy)ethoxy)ethyl methacrylate) (PTEGN<sub>3</sub>MA) with a degree of polymerization (DP) of 707, was prepared according to a procedure described previously (Scheme S1).<sup>36</sup> Poly(ethylene glycol) monomethyl ether polymers (CH<sub>3</sub>O-PEO-OH) with a molecular weight of 2,000, 5,000, and 750 g/mol (Aldrich) were end functionalized with an alkyne group by a N-(3dimethylaminopropyl)-N'-ethylcarbodiimide hydrochloride-catalyzed coupling reaction with 4pentynoic acid, yielding alkyne end-functionalized PEO-2k, PEO-5k, and PEO-750, respectively.<sup>36</sup> Cinnamoyl chloride (98%, predominantly trans) was purchased from Fisher Scientific/Acros and used as received. 2-(t-Butyldimethylsilyloxy)ethyl acrylate (SiEA) was prepared from 2-hydroxyethyl acrylate and t-butyldimethylsilyl chloride, and the molecular structure was confirmed by <sup>1</sup>H NMR spectroscopy analysis. Methoxytri(ethylene glycol) acrylate (TEGMA) was synthesized by the reaction of tri(ethylene glycol) monomethyl ether and acryloyl chloride. 45 Propargyl 2-bromoisobutyrate was synthesized as described previously. 36 All other chemicals were purchased from either Aldrich or Fisher and used as received.

Characterization. Size exclusion chromatography (SEC) of molecular bottlebrush samples and backbone polymer PTEGN<sub>3</sub>MA was performed at 50 °C using a PL-GPC 50 Plus (an integrated GPC/SEC system from Polymer Laboratories, Inc.) with a differential refractive index detector, one PLgel 10 μm guard column (50 × 7.5 mm, Agilent Technologies), and three PLgel 10 μm mixed-B columns (each 300 × 7.5 mm, linear molecular weight range from 500 to 10,000,000 Da, Agilent Technologies). The data were processed using Cirrus<sup>TM</sup> GPC/SEC

software (Polymer Laboratories, Inc.). *N,N*-Dimethylformamide (DMF) with 50 mM LiBr was used as the eluent at a flow rate of 1.0 mL/min. SEC of backbone polymer precursors and side chain polymers was carried out using a PL-GPC 20 integrated GPC/SEC system from Polymer Laboratories, Inc. with a refractive index detector, one PLgel 5 μm guard column (50 × 7.5 mm, Agilent Technologies), and two PLgel 5 μm mixed-C columns (each 300 × 7.5 mm, linear molecular weight range from 200 to 2,000,000 Da, Agilent Technologies). THF was used as the solvent at a flow rate of 1.0 mL/min. Both SEC systems were calibrated with linear polystyrene standards (Scientific Polymer Products, Inc.). <sup>1</sup>H and <sup>13</sup>C NMR spectra were recorded on a Varian Mercury 300 or a Varian VNMRS 500 NMR spectrometer. UV-vis spectra were recorded using a T60U UV-Vis spectrophotometer equipped with a Peltier temperature controller system (PTC-2) in conjunction with UVWIN software version 6.1.0 (Persee Analytics, Inc.).

**Dynamic Light Scattering (DLS) Study of Thermoresponsive Molecular Bottlebrushes in Water.** DLS studies of thermoresponsive properties of molecular bottlebrushes in water were performed using a Malvern Zetasizer Nano ZS system with a He-Ne 633 nm laser and a temperature controller. The brush molecules were dissolved in Milli-Q water in an ice/water bath at a desired polymer concentration and then kept in a refrigerator (4 °C) for at least 15 h to ensure complete dissolution. The DLS samples with a polymer concentration of 0.2 mg/g were passed through a 0.2 μm PTFE filter at 22 °C, and no changes to the size and size distribution were observed after filtration. For UV-irradiated aqueous solutions of molecular bottlebrushes with concentrations of 10, 25, and 100 mg/g, the DLS samples were prepared by diluting the irradiated brush solutions with Milli-Q at ambient temperature and analyzed directly without filtration. The temperature was raised stepwise, and at each chosen temperature the DLS sample was equilibrated

for 5 min. The reported DLS sizes were Z-average hydrodynamic diameters, obtained by cumulant analysis using the Malvern Zetasizer software.

Atomic Force Microscopy (AFM) Study of Molecular Bottlebrushes Before and After UV Irradiation. A Digital Instruments Multimode IIIa Scanning Probe Microscope was employed to image molecular bottlebrushes on freshly cleaved bare mica or poly(methyl methacrylate) (PMMA)-coated, freshly cleaved mica, which was operated in tapping mode under ambient conditions. Reflective Al-coated Si probes with a nominal resonant frequency of 300 kHz and force constant of 40 N/m (Budget Sensors) were used. The AFM samples were prepared by spin casting of aqueous solutions of molecular brushes, either original brushes or UV-irradiated at 60 °C, with a concentration of 0.05 or 0.025 mg/g onto freshly cleaved mica or PMMA-coated mica at a spin speed of 3000 rpm (P-6000 Spin Coater, Specialty Coating Systems, Inc.). The aqueous solutions of molecular brushes were cooled in an ice/water bath or heated in an oven with a preset temperature of 60 or 65 °C prior to spin casting. For the preparation of AFM samples at 60 or 65 °C, the spin casting stage, mica disk, and glass pipette were also heated in an oven with a preset respective temperature. To coat mica with PMMA, three drops of a 1.0 mg/g solution of PMMA  $(M_n = 54.9 \text{ kDa}, \text{ dispersity } (D) = 1.06)$ , Polymer Standards Service GmbH) in CHCl<sub>3</sub> was deposited onto a freshly cleaved mica disc and spun at 3000 rpm. The quantitative image analysis was performed with ImageJ software.

Synthesis of Thermoresponsive, UV-Crosslinkable Poly(methoxytri(ethylene glycol) acrylate-co-2-cinnamoylethyl acrylate) (P(TEGMA-co-CEA)). Propargyl 2-bromoisobutyrate (31.4 mg, 0.153 mmol), TEGMA (2.715 g, 12.4 mmol), SiEA (0.725 g, 3.15 mmol), CuCl (13.7 mg, 0.138 mmol), PMDETA (58.9 mg, 0.340 mmol), and anisole (3.736 g) were weighed out into a 25 mL two-necked flask with a stir bar. The mixture was degassed immediately by three freeze-

pump-thaw cycles, and the flask was placed in an 85 °C oil bath. After 24 h, the temperature was increased to 90 °C. After the polymerization proceeded for a total of 44 h, the flask was taken out from the oil bath, and the mixture was passed through a neutral alumina (top)/silica gel (bottom) column. The polymer was purified by precipitation into hexanes three times. After drying under high vacuum, a light yellow, viscous polymer was obtained (1.089 g). The SEC results with THF as eluent:  $M_{n,SEC} = 9,300$  g/mol and dispersity (D) = 1.15. The total DP was calculated to be 43 based on the monomer conversion and the monomers-to-initiator ratio. The numbers of monomer units of TEGMA and SiEA were 34 and 9, respectively, determined by the <sup>1</sup>H NMR analysis of the purified copolymer P(TEGMA-co-SiEA) using the integrals of the peaks at 4.15 ppm (-COOC $H_2$ - of TEGMA units) and 4.05 ppm (-COOC $H_2$ - of SiEA units) (Figure S1).

P(TEGMA-co-SiEA) (1.013 g) was added into a 100 mL round bottom flask with a stir bar and dissolved in ethanol (8 g). HCl (1.0 M, 1.8 mL) was added dropwise over a period of 10 min, and the mixture was stirred for 3 h to cleave the silyl ether protective group. The volatiles were then removed under high vacuum, yielding a dried, yellow viscous polymer. The resultant copolymer was dissolved in CH<sub>2</sub>Cl<sub>2</sub> (5 mL) and placed in an ice/water bath under nitrogen. Triethylamine (1.219 g, 12.0 mmol) was added, followed by the dropwise addition of a solution of cinnamoyl chloride (0.760 g, 4.56 mmol) in CH<sub>2</sub>Cl<sub>2</sub> (5 mL) over a period of 10 min. The mixture was allowed to warm to room temperature and stirred overnight under nitrogen. The reaction mixture was then concentrated to ~ 2 mL, followed by the addition of pyridine (3 mL), dry THF (3 mL), and more cinnamoyl chloride (0.760 g, 4.56 mmol). The reaction continued for 2 more days under nitrogen atmosphere. The white solid precipitate was removed by vacuum filtration, and the polymer solution in THF was passed through a basic alumina (top)/silica gel (bottom) column twice, followed by precipitation in hexanes. The purified polymer, P(TEGMA-co-CEA),

was then dried under high vacuum (yield: 0.696 g). SEC results:  $M_{n,SEC} = 9,500$  g/mol and D = 1.25. <sup>1</sup>H NMR spectroscopy analysis showed that the functionalization with cinnamoyl chloride was essentially complete, using the integrals of the peaks at 4.15 ppm (-COOC $H_2$ - of TEGMA units) and 4.23-4.42 ppm (-COOC $H_2$ CH<sub>2</sub>OOC- of CEA units) (Figure S2).

Study of Thermoresponsive Property of P(TEGMA-co-CEA) in Water. The transmittance of a 1.0 mg/g aqueous solution of P(TEGMA-co-CEA) at the wavelength of 500 nm was recorded as a function of temperature using a UV-vis spectrometer. The temperature was changed in a stepwise fashion, and at each selected temperature, the solution was equilibrated for 2 min. The LCST of P(TEGMA-co-CEA) was determined to be 27 °C with a range of 23 to 33 °C (Figure S3). The LCST transition was somewhat broadened, likely due to the compositional variations among the polymer chains. A hysteresis was observed for the heating and cooling processes, possibly because the  $\pi$ - $\pi$  stacking induced the association of cinnamate groups in the copolymer.

Synthesis of Binary Heterografted Molecular Bottlebrushes Composed of PEO and P(TEGMA-co-CEA). Described below is the synthesis and purification for the binary molecular bottlebrushes composed of PEO with a molecular weight of 5,000 g/mol and P(TEGMA-co-CEA) (MBB-5k). PTEGN<sub>3</sub>MA (10.21 mg, from a stock solution, 0.0420 mmol repeat units) was weighed out into an 8 mL vial with a stir bar. THF was evaporated using nitrogen flow, and DMF (1 mL) was added. Alkyne end-functionalized PEO-5k (126.2 mg, 0.0247 mmol) and P(TEGMA-co-CEA) (241.74 mg, from a stock solution, 0.0247 mmol) were added into a separate vial and transferred to the reaction vial using DMF (5 mL). CuCl (4.8 mg, 0.0485 mmol) was added, and the vial was sealed with a septum and flushed with nitrogen via needles for 10 min. PMDETA (10 μL) was injected via a microsyringe to start the reaction. After 16 h, benzyl propargyl ether (25 μL) was injected, and the reaction was allowed to proceed for additional 2 h. SEC analysis with the use of

mixed-B columns showed that  $M_{n,SEC}$  was 1,361,000 g/mol and D = 1.15. Based on the peak areas of molecular bottlebrushes (75.13%) and remaining side chain polymers (24.87%), the grafting density was calculated to be 87.6 %. The reaction mixture was diluted with THF and passed through silica gel/neutral alumina using CH<sub>2</sub>Cl<sub>2</sub> as eluent to remove the copper catalyst. The brushes were concentrated and purified by centrifugal filtration using a centrifuge tube with 50 kDa MWCO dialysis membrane (EMD Millipore Amicon Ultra-15 centrifugal filter unit) and a mixture of water and methanol (50:50, v/v) as a solvent. After five-to-six rounds of centrifugation and dissolution, the unreacted side chain polymers were completely removed, as confirmed by SEC analysis.  $M_{n,SEC}$  of the purified brushes was 1,397,000 g/mol, and the D was 1.15. The yield of BMB-5k was 260 mg. <sup>1</sup>H NMR analysis (Figure S4), using the integrals of the peaks at 4.04-4.42 ppm (-COOCH<sub>2</sub>- of P(TEGMA-co-CEA)) and 3.54-3.66 ppm (-OCH<sub>2</sub>CH<sub>2</sub>- of PEO and -COOCH<sub>2</sub>CH<sub>2</sub>OCH<sub>2</sub>CH<sub>2</sub>OCH<sub>2</sub>CH<sub>2</sub>OCH<sub>3</sub> of P(TEGMA-co-CEA)), showed that the molar ratio of PEO-5k and P(TEGMA-co-CEA) in BMB-5k was 52 : 48, close to that in the feed (50 : 50).

The binary molecular brushes composed of PEO-2k and P(TEGMA-co-CEA) (BMB-2k) were synthesized and purified via the same procedure as for BMB-5k. From the SEC analysis of the final reaction mixture, the grafting density was calculated to be 82.7%. After the purification,  $M_{n,SEC}$  was 1,146,000 g/mol, and D was 1.16.  $^{1}$ H NMR spectroscopy showed that the actual molar ratio of PEO-2k and P(TEGMA-co-CEA) in the brushes BMB-2k was 52 : 48 (Figure S5).

BMB-750 molecular bottlebrushes were prepared from alkyne end-functionalized PEO-750 and P(TEGMA-co-CEA) by the same method using the same PEO-to-P(TEGMA-co-CEA) and alkyne-to-azide molar ratios as for BMB-5k and -2k. The grafting density was 93.5%, calculated from the peak areas of the brushes (81.14 %) and side chain polymers in the SEC analysis.  $M_{n,SEC}$ 

was 1,194,000 g/mol and the D was 1.15. From <sup>1</sup>H NMR analysis, the molar ratio of PEO-750 and P(TEGMA-co-CEA) side chains was 53 : 47 (Figure S6).

UV Crosslinking of Thermo- and Light-Responsive Molecular Bottlebrushes in Water at Various Concentrations at 60 °C. The molecular brushes were crosslinked in the collapsed state at 60 °C via photocoupling of cinnamate groups using short wavelength (254 nm) UV light from a handheld TLC lamp/detector. The conversion of cinnamate groups was determined from the decrease in the cinnamate's absorbance at 278 nm. The absorbance of a 0.2, or 0.1 or 0.05 mg/g brush solution before irradiation was used as reference, and the more concentrated solutions were diluted to the reference concentration for UV-Vis spectroscopy analysis.

#### **Results and Discussion**

The thermoresponsive, UV-crosslinkable binary heterografted molecular bottlebrushes (BMB-5k) composed of 5 kDa PEO (DP = 114) and P(TEGMA-co-CEA) with a DP of 43 were synthesized by co-grafting alkyne end-functionalized PEO and P(TEGMA-co-CEA) in a molar ratio of 1 : 1 onto azide-bearing backbone polymer PTEGN<sub>3</sub>MA with a DP of 707 via copper(I)-catalyzed azide-alkyne cycloaddition click reaction. SEC analysis showed that after purification the  $M_{n,SEC}$  of BMB-5k was 1,397,000 g/mol and the D was 1.15, relative to polystyrene standards. By using the peak area ratio of molecular brushes and unreacted side chain polymers from the SEC chromatogram of the reaction mixture at the end of the reaction, the grafting density was calculated to be 87.6%. $^{36,37}$  <sup>1</sup>H NMR spectroscopy analysis showed that the molar ratio of grafted PEO to P(TEGMA-co-CEA) in BMB-5k was 52 : 48, close to the feed ratio of 50 : 50.

The thermoresponsive, UV-crosslinkable side chain polymer, P(TEGMA-co-CEA), was prepared by atom transfer radical copolymerization of methoxytri(ethylene glycol) acrylate

(TEGMA) and 2-(*t*-butyldimethylsilyloxy)ethyl acrylate using propargyl 2-bromoisobutyrate as initiator and subsequent removal of the silyl protecting group and installation of cinnamate via esterification reaction. The DP of the alkyne end-functionalized P(TEGMA-*co*-CEA) was 43, with 34 TEGMA units and 9 CEA units. This copolymer exhibited a cloud point of 27 °C with a transition ranging from 23 to 33 °C in water at a concentration of 1.0 mg/g, which is significantly lower than that of the homopolymer of TEGMA in water (58 °C)<sup>45-47</sup> due to the introduction of hydrophobic groups. As Considering that there are three bonds in one repeat unit in PEO and two bonds in one monomer unit in P(TEGMA-*co*-CEA), the contour chain length of 5 kDa PEO is significantly greater than that of P(TEGMA-*co*-CEA) (by about 4 times). The cinnamate groups incorporated into the thermoresponsive polymer can undergo a [2 + 2] cycloaddition reaction upon irradiation with 254 nm UV light, Allowing for crosslinking of collapsed brushes at higher temperatures and subsequent morphology characterization under ambient conditions by AFM.

For comparison, we synthesized two additional heterografted molecular brushes, BMB-2k and BMB-750, using the same thermoresponsive, UV-crosslinkable polymer, P(TEGMA-co-CEA), but lower molecular weight PEO polymers (2k Da for BMB-2k, DP = 45; 750 Da for BMB-750, DP = 17). The grafting density and the molar ratio of two side chain polymers in each sample are comparable to those of BMB-5k. The molecular characteristics for these three brush samples are summarized in Table 1. Note that the  $M_{n,SEC}$  of BMB-750 is slightly larger than that of BMB-2k, likely because of the much larger increase in the high molecular weight shoulder after purification due to the loss of some lower molecular weight brush molecules (Figure S6A).

**Table 1.** Characterization Data for Three Heterografted Molecular Bottlebrush Samples Composed of PEO and Thermoresponsive, UV-Crosslinkable P(TEGMA-co-CEA) Side Chains

Molecular	PEO M <sub>n</sub> ; DP	P(TEGMA-co-	$M_{n,SEC}$ a	$D^{\mathrm{a}}$	Grafting	PEO to P(TEGMA-co-
Brushes		CEA)			Density b	CEA) Molar Ratio <sup>c</sup>
BMB-5k	5 kDa; 114	DP = 43 (34, 9)	1 397 000	1.15	87.6%	52:48

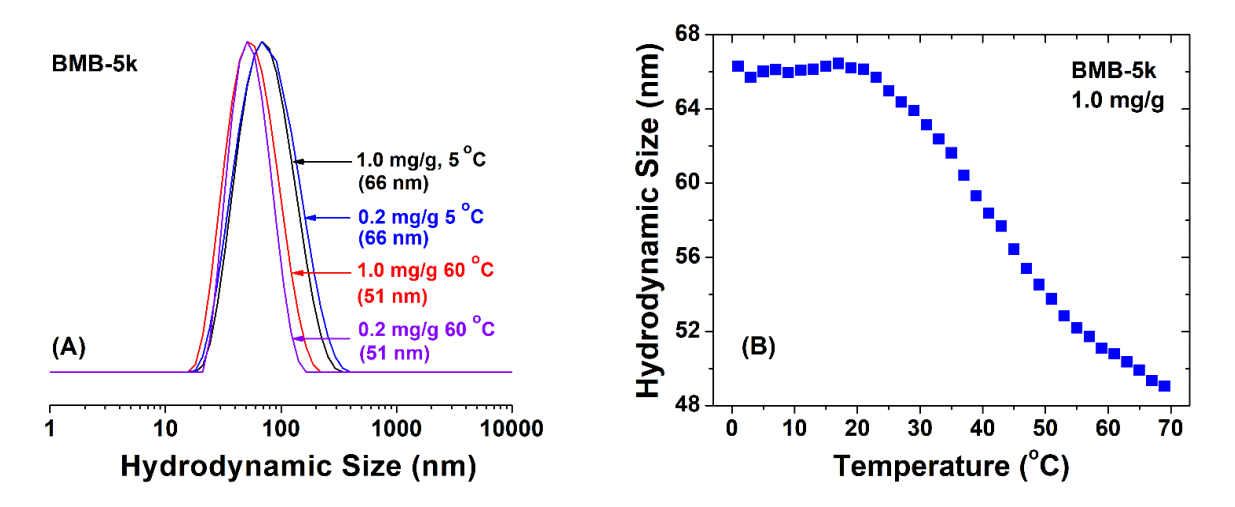
BMB-2k	2 kDa; 45	DP = 43 (34, 9)	1 146 000	1.16	82.7%	52:48
BMB-750	750 Da; 17	DP = 43 (34, 9)	1 194 000	1.15	93.5%	53:47

<sup>&</sup>lt;sup>a</sup> The number average molecular weight  $(M_{n,SEC})$  and dispersity (D) were determined by size exclusion chromatography (SEC) using narrow disperse polystyrene standards for calibration. <sup>b</sup> Grafting density was calculated from the peak area ratio of molecular brushes and unreacted side chains from the SEC chromatograph of the reaction mixture. <sup>c</sup> The molar ratio of two side chain polymers was determined from <sup>1</sup>H NMR spectrum.

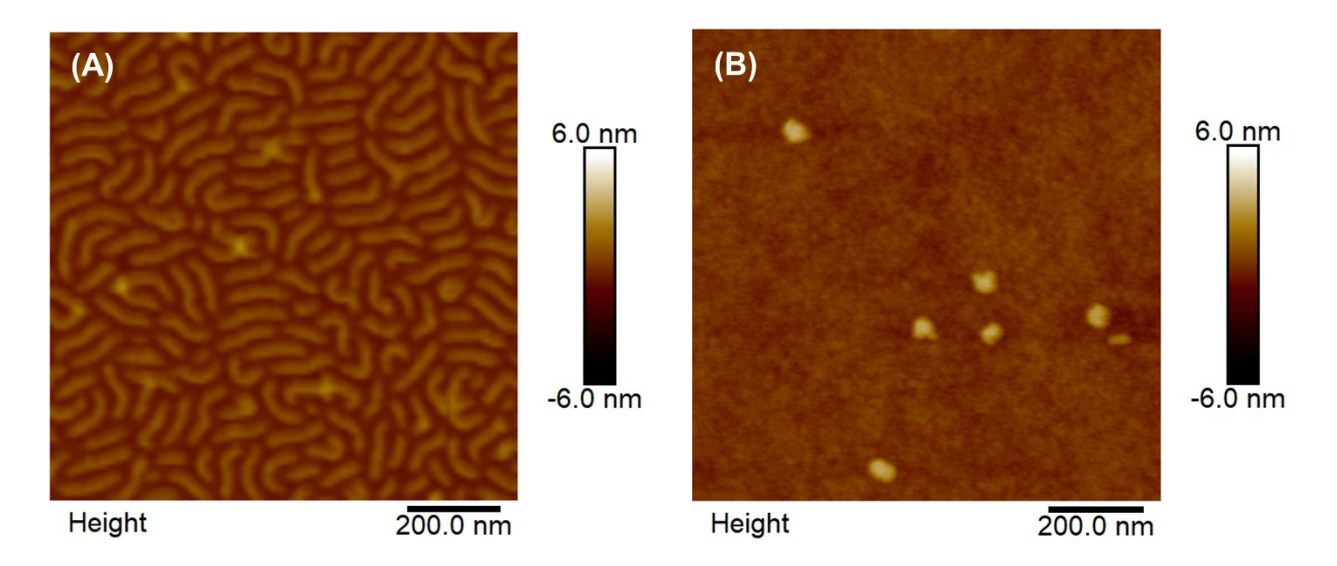
The thermoresponsive property of BMB-5k in water was first investigated by DLS. At a concentration of either 0.2 or 1.0 mg/g, a single distribution was observed at both 5 and 60 °C, with an average apparent hydrodynamic size  $(D_h)$  of 66 nm and 51 nm, respectively (Figure 1A). The polydispersity index (PDI) values of the size distributions at 5 °C were 0.220 and 0.255 for the concentrations of 0.2 mg/g and 1.0 mg/g, respectively, while at 60 °C they were 0.181 and 0.197, respectively. The fact that the sizes and distributions of BMB-5k are essentially the same at concentrations of 0.2 and 1.0 mg/g at either 5 or 60 °C indicated intramolecular collapse of thermoresponsive brush molecules at both concentrations, consistent with our previous observation of the stabilization effect of PEO side chains.<sup>36</sup> Note that on the basis of the D<sub>h</sub> value of BMB-5k at 5 °C the overlap concentration was estimated to be 0.0516 g/mL (see Page S5 in the Supporting Information). Figure 1B shows the  $D_h$  of BMB-5k in water at the concentration of 1.0 mg/g as a function of temperature upon heating. The D<sub>h</sub> decreased gradually from 66 nm at 5 °C to 51 nm at 60 °C and then 49 nm at 69 °C, suggesting that the BMB-5k brush molecules changed to a more compact conformation with PEO corona stabilizing the collapsed P(TEGMA-co-CEA) side chains upon heating. Compared with the transmittance change from  $\sim 100$  to  $\sim 0\%$  of the P(TEGMA-co-CEA) copolymer in water at a concentration of 1.0 mg/g, which occurred over a temperature range of ~ 10 °C (Figure S3), the hydrodynamic size transition of BMB-5k brushes was significantly broader, spanning a temperature range of ~ 40 °C, although the onset temperature

was about the same (22 °C). This is likely a result from the combined effects of the shrinking of PEO side chains at elevated temperatures and the compositional variations of P(TEGMA-co-CEA) as well as the heterogeneity in the distribution of two side chain polymers along the backbone of molecular brushes.

The decrease in D<sub>h</sub> upon heating observed from DLS measurements suggested a thermallyinduced worm-to-sphere transition of BMB-5k, which was confirmed by AFM study. Figure 2A shows a representative AFM image of BMB-5k brush molecules spin cast onto poly(methyl methacrylate) (PMMA)-coated mica from a 0.05 mg/g aqueous solution at 0 °C; as expected, a wormlike morphology was observed. Image analysis using the NIH ImageJ software showed that the average contour length of the worms was  $128 \pm 29$  nm, with a typical height of  $\sim 1$  nm (Figure S7). A fully extended brush molecule with a backbone DP of 707 in an all-trans conformation would have a length of 180 nm, indicating a degree of stretching of 71%. In contrast, nearly spherical nano-objects with an average size of  $49 \pm 8$  nm and a typical height of 3.5 nm were seen in the sample spin cast from an aqueous solution of BMB-5k with a concentration of 0.025 mg/g at 65 °C (Figure 2B and Figure S8), evidencing the thermally induced shape transition of brush molecules from wormlike to spherical. Note that we used PMMA-coated mica instead of freshly cleaved mica to prepare AFM samples of BMB-5k at 0 and 65 °C, because we found that the collapsed globular nano-objects of molecular bottlebrushes at higher temperatures were unfolded on freshly cleaved mica due to the strong attractive interactions of 5k PEO side chains with hydrophilic mica surface (see Figures S9 and S10 in the Supporting Information).



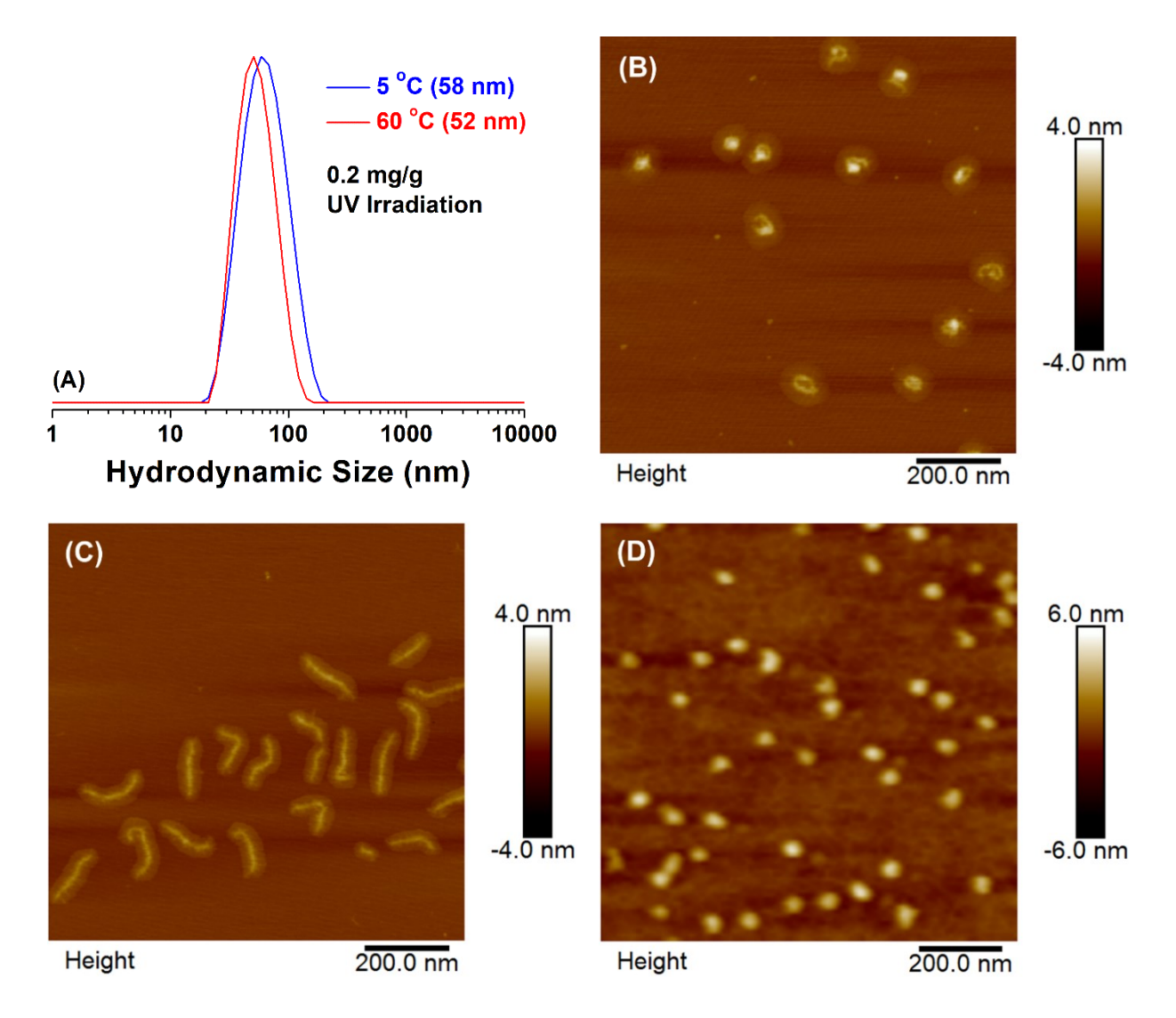
**Figure 1.** (A) Hydrodynamic size ( $D_h$ ) distribution from DLS measurements at 5 and 60 °C for BMB-5k in water at concentrations of 0.2 and 1.0 mg/g. (B) Plot of  $D_h$  of BMB-5k in water at a concentration of 1.0 mg versus temperature from a heating process.



**Figure 2.** AFM images of BMB-5k brushes spin cast on PMMA-coated mica from an aqueous solution with a BMB-5k concentration of 0.05 mg/g at 0 °C (A) and of 0.025 mg/g at 65 °C (B).

The 0.2 mg/g aqueous solution of BMB-5k was then irradiated in the collapsed spherical state at 60 °C with 254 nm UV light until the conversion of cinnamate groups reached 40% (Figure S11), which was calculated from the intensity decrease of the cinnamate's absorbance peak at 278 nm before and after the irradiation. From the DLS measurements, the  $D_h$  at 5 °C decreased from 66 nm (before the UV irradiation) to 58 nm with a PDI of 0.183 (Figure 3A), and the one size

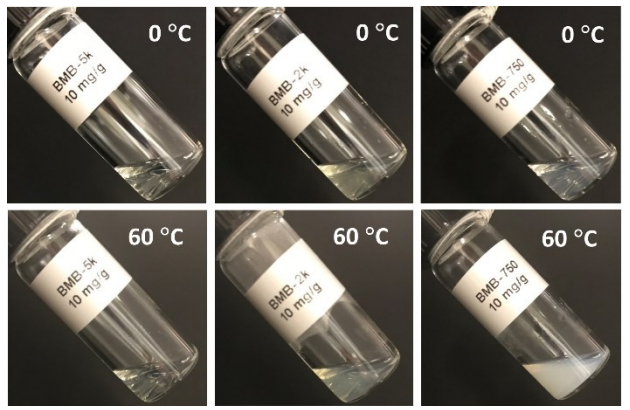
distribution was maintained, whereas the  $D_h$  at 60 °C (52 nm), with a single size distribution (PDI = 0.186), was essentially the same as that before UV irradiation (51 nm). For AFM analysis, the irradiated brush solution was diluted to 0.05 mg/g, equilibrated in an ice/water bath, and then spin cast onto freshly cleaved bare mica; a spherical morphology was observed with a coiled backbone being in the center of each molecule and the PEO side chains spreading out on mica (Figure 3B). The average diameter of the molecules in Figure 3B was 97  $\pm$  8 nm; from the cross-sectional analysis, the height of the backbone was in the range of 1.3 - 1.8 nm, and the thickness of PEO corona was ~ 0.4 nm (Figure S12). This is in contrast to the wormlike morphology of BMB-5k spin cast on freshly cleaved mica at 0 °C before the UV irradiation (Figure 3C), which exhibited a length of  $142 \pm 36$  nm. Interestingly, the thicknesses of the backbone and the PEO corona of the worms in Figure 3C (Figure S13) were the same as those in Figure 3B. Clearly, the collapsed P(TEGMA-co-CEA) side chains were intramolecularly crosslinked in the core of each brush molecule at 60 °C by UV light, and the spherical shape was fixed. A similar morphology was observed by AFM when the crosslinked brushes were spin cast onto mica at 60 °C (Figure S14). Figure 3D shows an AFM image of the crosslinked BMB-5k spun cast on PMMA-coated mica from a 0.05 mg/g solution at 0 °C; the brush molecules were in a globular morphology even at a temperature below the LCST (Figure S15), and the average size was  $46 \pm 7$  nm. We also imaged the crosslinked BMB-5k on PMMA-coated mica prepared from an aqueous solution at 60 °C and found that the size was  $45 \pm 8$  nm (Figure S16). These sizes were very close to that of BMB-5k on PMMA at 65 °C (49  $\pm$  8 nm, Figures 2B & S8).



**Figure 3.** (A) Hydrodynamic size ( $D_h$ ) distributions at 5 and 60 °C from DLS measurements for a 0.2 mg/g BMB-5k in water irradiated with 254 nm UV light to a 40% conversion of cinnamate groups. (B) and (D) AFM images of the UV-crosslinked BMB-5k spin cast on freshly cleaved mica and PMMA-coated mica, respectively, from a 0.05 mg/g solution at 0 °C, diluted from the irradiated, 0.2 mg/g solution. (C) AFM height image of BMB-5k spin cast onto freshly cleaved mica from a 0.05 mg/g aqueous solution at 0 °C.

Like BMB-5k, BMB-2k and -750 also exhibited thermally induced shape transitions from wormlike to globular in dilute aqueous solutions upon heating, as shown in the AFM images of these brushes spin cast on PMMA-coated mica from 0.05 mg/g aqueous solutions equilibrated at 0 and 65 °C (see Figures S17-S20 in the Supporting Information). All of these three molecular

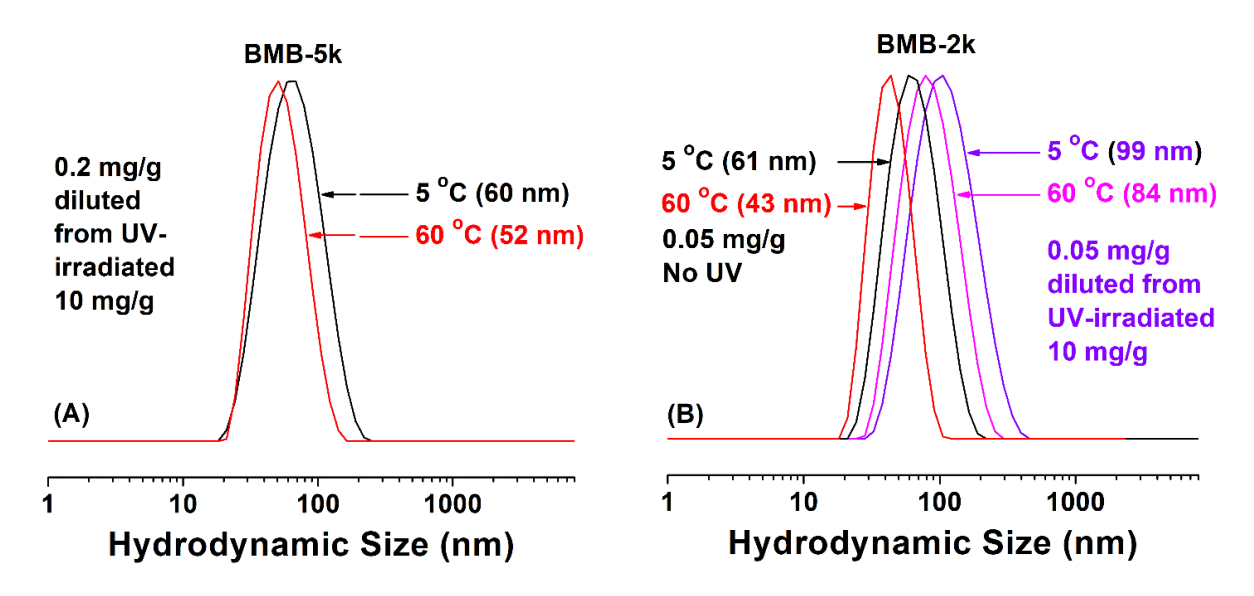
brushes contained PEO side chains but with different chain lengths (DP = 114, 45, and 17, respectively), and the molar ratios of PEO to P(TEGMA-co-CEA) side chains in the brushes were about the same (52 : 48 for BMB-5k and -2k, and 53 : 47 for BMB-750). We hypothesized that the stabilization abilities of these PEO polymers for the collapsed state of molecular bottlebrushes in more concentrated solutions would be different because of their different chain lengths. To compare their solution behaviors, we made an aqueous solution with a concentration of 10 mg/g for each of these three brush samples. Figure 4 shows the photos of three 10 mg/g solutions at  $\sim$  0 and 60 °C. While the BMB-5k stayed clear and no change in the appearance was observed upon heating from 0 to 60 °C, a slight blue tinge developed for the BMB-2k solution. In stark contrast, the BMB-750 solution turned cloudy, indicating that the short PEO in BMB-750 cannot prevent the intermolecular aggregation of the brush molecules at this concentration after the collapse of P(TEGMA-co-CEA) side chains at temperatures above the LCST transition.



**Figure 4.** Optical photos of 10 mg/g aqueous solutions of BMB-5k, BMB-2k, and BMB-750 in 4.0 mL vials at 0 °C (top row) and 60 °C (bottom row).

Although one can simply dilute the 10 mg/g aqueous solutions of BMB-5k and -2k at 60 °C to an appropriate concentration for DLS and AFM measurements to examine if the heating-induced transition occurred intramolecularly or intermolecularly, a main concern is that the dilution with

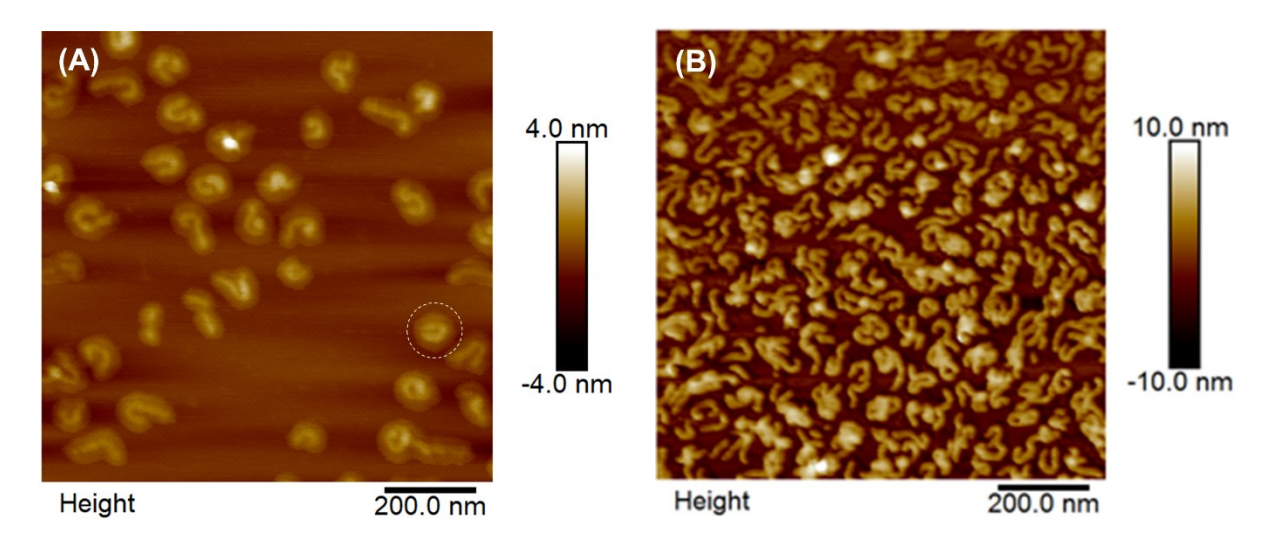
Milli-Q water might cause the dissociation of aggregates if present. This was why we introduced UV-crosslinkable cinnamate groups into thermoresponsive side chains, which made it possible to crosslink the collapsed thermoresponsive side chains and thus fix the shape at temperatures above the LCST. The 10 mg/g aqueous solutions of BMB-5k and -2k were irradiated in the collapsed state at 60 °C with 254 nm UV light until a cinnamate conversion of 32% for BMB-5k (Figure S21) and 35% for BMB-2k (Figure S22) was reached. After diluting the solutions to the concentration of 0.2 mg/g, DLS measurements showed that for BMB-5k the hydrodynamic sizes at 5 and 60 °C were 60 (PDI = 0.233) and 52 nm (PDI = 0.202), respectively, with a single size distribution at each temperature (Figure 5A), which were very close to or the same as the  $D_h$  values (58 and 52 nm, respectively) for the UV irradiated, 0.2 mg/g solution of BMB-5k. This suggests a worm-to-sphere shape changing of BMB-5k molecules at a concentration of 10 mg/g upon heating from below the LCST to 60 °C before the UV irradiation. In contrast, the D<sub>h</sub> values at 5 and 60 °C of the UV-crosslinked BMB-2k in water at a concentration of 0.05 mg/g, diluted from the irradiated, 10 mg/g solution, were 99 (PDI = 0.294) and 84 nm (PDI = 0.278), respectively, much larger than those of the non-UV-irradiated BMB-2k at a concentration of 0.05 mg/g (61 and 43 nm, respectively, with PDI values of 0.259 and 0.191) (Figure 5B). For comparison, we irradiated the 0.05 mg/g solution of BMB-2k at 60 °C with UV light to a cinnamate conversion of 42% (Figure S23); DLS analysis showed that the  $D_h$  values at 5 and 60 °C were 49 (PDI = 0.150) and 42 nm (PDI = 0.162), respectively (Figure S24). Thus, the larger hydrodynamic sizes for the irradiated, 10 mg/g solution of BMB-2k suggested intermolecular aggregation and crosslinking at this concentration. We also attempted to irradiate the 10 mg/g solution of BMB-750 at 60 °C, however, a white precipitate was formed and could not be re-dissolved in water.



**Figure 5.** Apparent hydrodynamic size ( $D_h$ ) distribution at 5 and 60 °C for (A) a 0.2 mg/g aqueous solution of irradiated BMB-5k, diluted from the UV-irradiated, 10 mg/g solution of BMB-5k and (B) a 0.05 mg/g aqueous solution of the irradiated BMB-2k, diluted from the UV-irradiated, 10 mg/g solution of BMB-2k, along with a 0.05 mg/g solution of unirradiated BMB-2k.

The difference between the UV-irradiated BMB-5k and -2k at the concentration of 10 mg/g can be clearly seen from AFM images (Figures 6, S25, and S26) of brush molecules spin cast on bare mica from the diluted solutions with a concentration 0.05 mg/g at 0 °C. For BMB-5k, the brushes were well separated from each other, and no intermolecular crosslinking was found. Moreover, most of the molecules were coiled and assumed a roughly spherical shape, though not all of them, likely because of the lower cinnamate conversion (32%) compared with that (40%) for Figure 3B. The size of a typical spherical molecule on bare mica, highlighted by a white, dashed circle in Figure 6A, is 91 nm, which is similar to that of the brush molecules in the UV-crosslinked, 0.2 mg/g sample shown in Figure 3B. When spin cast on PMMA-coated mica at 0 °C, spherical nano-objects with an average size of  $45 \pm 8$  nm were observed from AFM as expected (Figure S27). Thus, both DLS and AFM studies showed intramolecular crosslinking for BMB-5k in water at the concentration of 10 mg/g, indicating that the brushes molecules collapsed individually and transformed into a globular state. In stark contrast, the UV-irradiated BMB-2k brush molecules

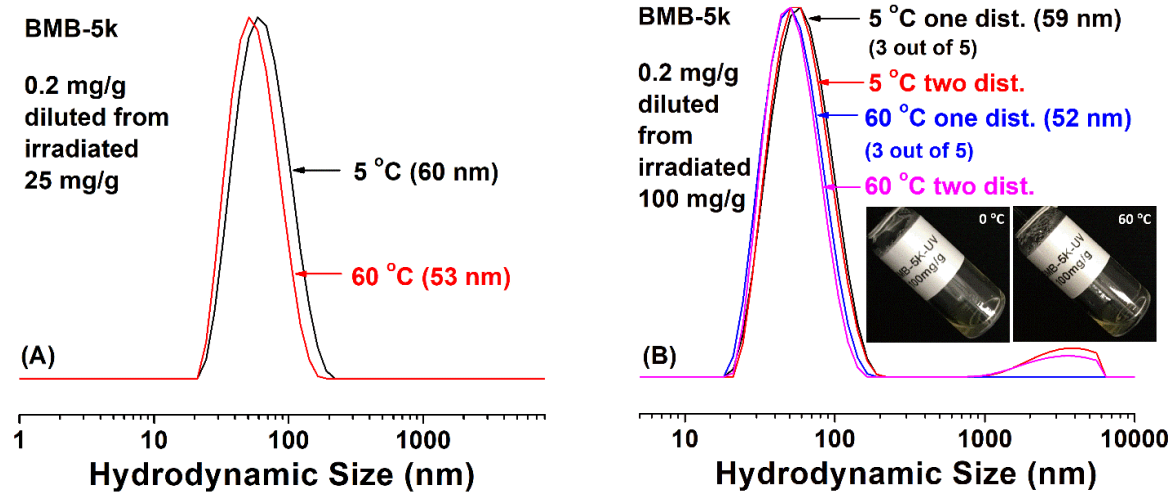
clumped together on freshly cleaved mica (Figure 6B). Note that the non-UV-irradiated BMB-2k assumed a wormlike shape on mica at 0 °C (Figure S28). Clearly, at the concentration of 10 mg/g, BMB-2k molecular bottlebrushes underwent intermolecular association upon heating above the LCST of P(TEGMA-*co*-CEA) side chains.



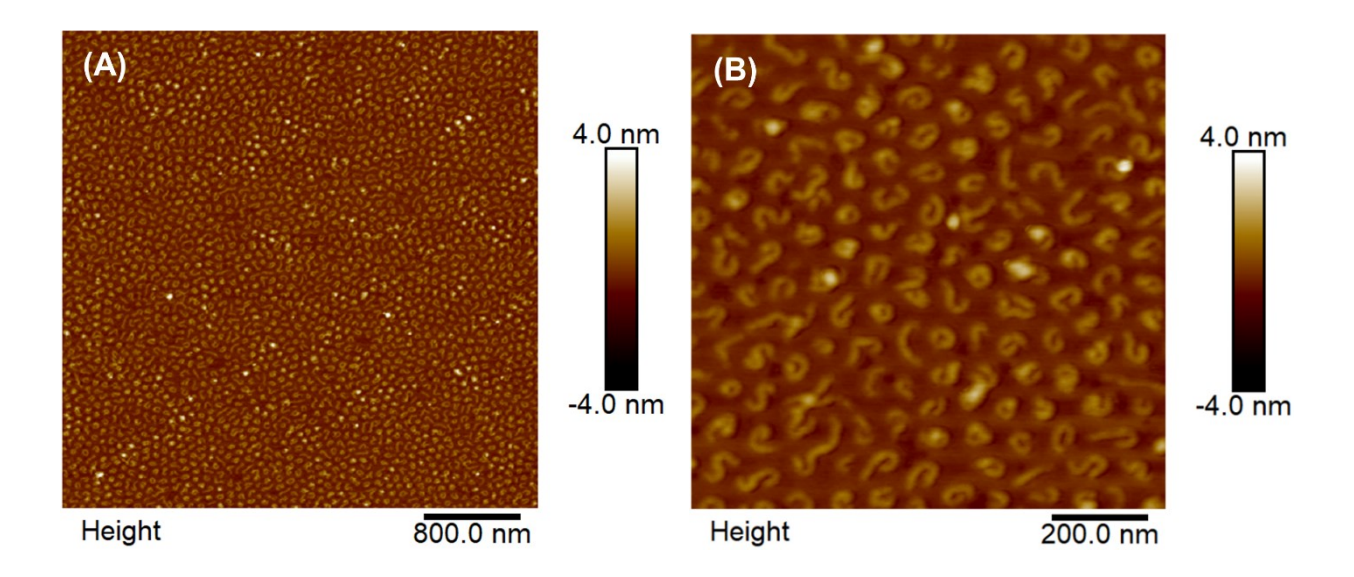
**Figure 6.** AFM image of (A) irradiated BMB-5k spin cast on freshly cleaved mica from a 0.05 mg/g aqueous solution at 0 °C, diluted from the UV irradiated, 10 mg/g BMB-5k solution, and (B) irradiated BMB-2k spin cast on freshly cleaved mica from a 0.05 mg/g aqueous solution at 0 °C, diluted from the UV irradiated, 10 mg/g BMB-2k solution.

To test how high the concentration of BMB-5k in water can be while maintaining worm-to-sphere shape changing, we further increased the brush concentration to 25 mg/g and 100 mg/g and irradiated the solutions with 254 nm UV light until the cinnamate conversion reached 29% (Figure S29) and 36% (Figure S30), respectively. The UV-irradiated aqueous solutions were then diluted to 0.2 mg/g for DLS measurements and 0.05 mg/g for preparing AFM samples. For the 25 mg/g sample, a single size distribution was observed at both 5 and 60 °C (Figure 7A), with an average hydrodynamic size of 60 (PDI = 0.200) and 53 nm (PDI = 0.186), respectively, which were essentially the same as those for the UV-irradiated 10 mg/g solution (60 and 52 nm, respectively, Figure 5A). AFM showed that most of the crosslinked brush molecules on freshly cleaved mica

were compact globular with a coiled backbone (Figures 8A and B and S31), although some extended worms were observed, similar to the molecules in Figure 6A. These data showed intramolecular crosslinking at the concentration of 25 mg/g. Image analysis of the spheres spin cast onto PMMA-coated mica (Figure S32) revealed that the average size was  $49 \pm 9$  nm, similar to the sizes for BMB-5k without crosslinking at 65 °C ( $49 \pm 8$  nm) and UV-crosslinking at concentrations of 0.2 mg/g ( $46 \pm 7$  nm) and 10 mg/g ( $45 \pm 8$  nm).



**Figure 7.** Hydrodynamic size ( $D_h$ ) distribution at 5 and 60 °C for a 0.2 mg/g aqueous solution of the irradiated BMB-5k, diluted from the UV-irradiated, 25 mg/g solution (A) and 100 mg/g solution (B). The inset in (B) are photos of the irradiated, 100 mg/g aqueous solution of BMB-5k in a 2 mL glass vial at 0 and 60 °C.



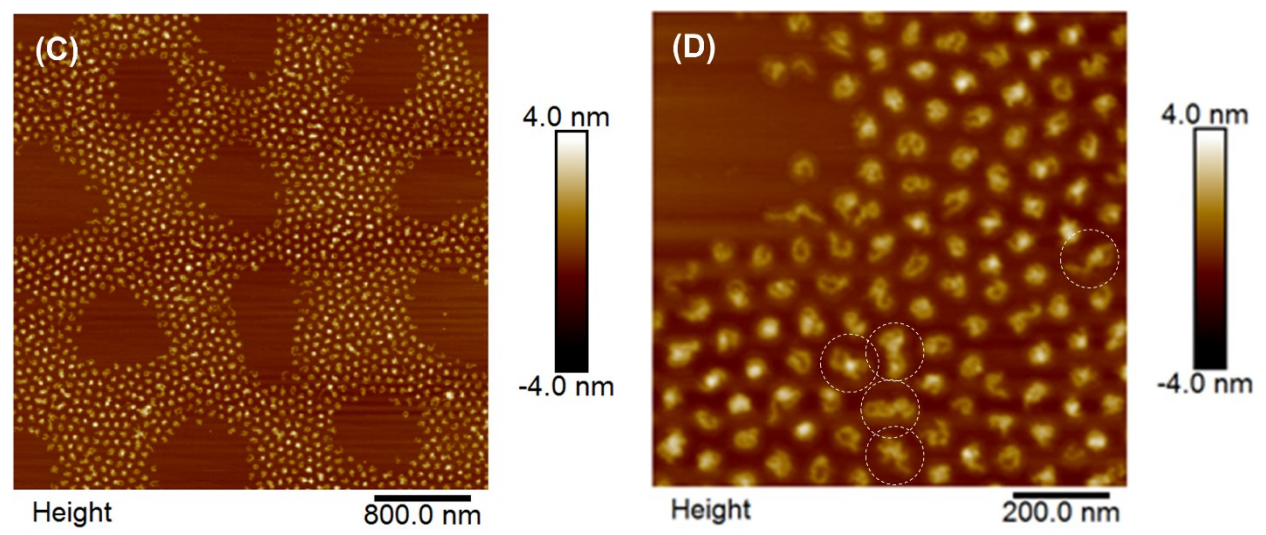


**Figure 8.** AFM height images of the crosslinked BMB-5k spin cast on freshly cleaved mica from a 0.05 mg/g aqueous solution at 0 °C, diluted from the UV irradiated, 25 mg/g solution ((A) and (B)) and 100 mg/g aqueous solution ((C) and (D)).

For the irradiated, 100 mg/g aqueous solution of BMB-5k, no change in the appearance was observed, and the solution in a small quantity in a 2 mL glass vial can be seen through at both 0 and 60 °C (see photos in Figure 7B). DLS of a 0.2 mg/g sample, diluted from the irradiated, 100 mg/g solution, showed a single size distribution in the majority of the measurements, with an average hydrodynamic size of 59 nm (PDI = 0.237) at 5 °C and 52 nm (PDI = 0.226) (Figure 7B). Occasionally, large species were observed in the size range of 1000 – 7000 nm. Note that each of five measurements shown in Figure 7B was an average of 10 runs and the DLS sample was not passed through a filter prior to the measurements. It is unclear what those large species were. Even if there were some loose intermolecular aggregates, the number should be quite small because the scattering intensity by DLS is heavily biased towards the large species. Figure 8C and D shows the AFM images of the irradiated BMB-5k brush molecules spin cast on freshly cleaved mica from the diluted solution with a concentration of 0.05 mg/g equilibrated at 0 °C. No large aggregates were observed (Figure S33); an overwhelming majority of brush molecules, if not 100%, collapsed from a wormlike to a compact globular shape and underwent UV-induced intramolecular

crosslinking. A few brush molecules in Figure 8D, indicated by a white, dashed circle, might be intermolecularly crosslinked, but it was also possible that these molecules stacked on each other or aggregated due to the spin casting in the AFM sample preparation process. By examining the AFM image in Figure 8D, no more than 5 out of 117 molecules were possibly intermolecularly crosslinked; thus at least 95% brush molecules underwent a wormlike-to-globular shape transition and intramolecular crosslinking by UV irradiation. From the AFM images of the diluted aqueous solution spin cast on PMMA-coated mica at 0 °C (Figure S34), the average size of the spheres was  $49 \pm 8$  nm, again similar to the irradiated BMB-5k molecular brushes at other concentrations. For the sample prepared on PMMA at 65 °C (Figure S35), the average size of the spheres was  $48 \pm 8$  nm.

#### **Conclusions**

Using three heterografted molecular brushes composed of a thermoresponsive, UV-crosslinkable polymer with a DP of 43 and PEO with different DPs (114, 45, or 17), we showed that thermally induced, worm-to-sphere shape changing can be achieved in moderately concentrated aqueous solution by increasing the protective PEO side chain length relative to that of the stimuli-responsive side chains. The brush polymers were prepared by grafting alkyne end-functionalized P(TEGMA-co-CEA) and PEO onto an azide-bearing backbone polymer via the azide-alkyne cycloaddition reaction. The incorporation of UV-crosslinkable cinnamate groups into the thermoresponsive side chains allowed for the photocrosslinking of collapsed brushes and the fixation of brushes' shape for more convenient characterization by AFM and DLS after dilution. At a concentration of 10 mg/g, the BMB-750 aqueous solution turned cloudy upon heating to 60 °C, indicating that the short PEO could not prevent the intermolecular association of brush

molecules. DLS and AFM studies showed that BMB-2k underwent intermolecular crosslinking in

a 10 mg/g aqueous solution at 60 °C. In contrast, BMB-5k exhibited worm-to-sphere shape

transitions at concentrations of 10 and 25 mg/g. Even at a concentration of 100 mg/g, AFM analysis

showed that ≥95% of brush molecules underwent intramolecular collapse and crosslinking. Given

that the conformational switching of molecular brushes has been restricted to dilute conditions or

at interfaces, we believe that the method reported here for achieving shape transitions between

wormlike and globular in moderately concentrated solutions will enable a plethora of new

opportunities for potential applications of shape changing molecular brushes such as drug delivery,

viscosity modification, lubrication, etc., and further advance the field of molecular bottlebrushes.

**Acknowledgements:** The authors thank NSF (DMR-1607076 and CHE-1709663) for the support.

**Supporting Information Available** 

The Supporting Information is available free of charge on the ACS Publications website at DOI:

10.1021/xxxxxxxx. Characterization of side chain polymers and molecular brushes, estimation of

overlap concentration of BMB-5k, UV-vis spectra after UV-crosslinking of molecular brushes at

various concentrations, additional AFM images of BMB-5k, -2k, -750 under various conditions

and DLS data.

**Author Information** 

Corresponding Author

\*E-mail: bzhao@utk.edu (B.Z.)

**ORCID** 

Bin Zhao: 0000-0001-5505-9390

Notes

The authors declare no competing financial interest.

26

#### References

- 1. Lodish, H.; Berk, A.; Zipursky, S. L.; Matsudaira, P.; Baltimore, D.; Darnell, J. *Molecular Cell Biology*, 4th ed. New York: W. H. Freeman; 2000.
- 2. Alexander-Katz, A. Toward Novel Polymer-Based Materials Inspired in Blood Clotting. *Macromolecules* **2014**, *47*, 1503–1513.
- 3. Schneider, S. W.; Nuschele, S.; Wixforth, A.; Gorzelanny, C.; Alexander-Katz, A.; Netz, R. R.; Schneider; M. F. Shear-Induced Unfolding Triggers Adhesion of von Willebrand Factor Fibers. *Proc. Natl. Acad. Sci. U. S. A.* **2007**, *104*, 7899-7903.
- 4. Lavalle, P.; Boulmedais, F.; Schaaf, P.; Jierry, L. Soft-Mechanochemistry: Mechanochemistry Inspired by Nature. *Langmuir* **2016**, *32*, 7265-7276.
- 5. Yao, M.; Goult, B. T.; Klapholz, B.; Hu, X.; Toseland, C. P.; Guo, Y.; Cong, P.; Sheetz, M. P.; Yan, J. The Mechanical Response of Talin. *Nature Commun.* **2016**, *7*, 11966, DOI: 10.1038/ncomms11966.
- 6. Zhang, M. F.; Müller, A. H. E. Cylindrical Polymer Brushes. *J. Polym. Sci. Part A: Polym. Chem.* **2005**, *43*, 3461-3481.
- 7. Verduzco, R.; Li, X.; Pesek, S. L.; Stein, G. E. Structure, Function, Self-Assembly, and Applications of Bottlebrush Copolymers. *Chem. Soc. Rev.* **2015**, *44*, 2405–2420.
- 8. Xia, Y.; Olsen, B. D.; Kornfield, J. A.; Grubbs, R. H. Efficient Synthesis of Narrowly Dispersed Brush Copolymers and Study of Their Assemblies: The Importance of Side Chain Arrangement. *J. Am. Chem. Soc.* **2009**, *131*, 18525-18532.
- 9. Li, Z.; Ma, J.; Cheng, C.; Zhang, K.; Wooley, K. L. Synthesis of Hetero-Grafted Amphiphilic Diblock Molecular Brushes and Their Self-Assembly in Aqueous Medium. *Macromolecules* **2010**, *43*, 1182-1184.
- 10. Wang, J.; Lu, H.; Ren, Y.; Zhang, Y.; Morton, M.; Cheng, J.; Lin, Y. Interrupted Helical Structure of Grafted Polypeptides in Brush-Like Macromolecules. *Macromolecules* **2011**, *44*, 8699–8708.
- 11. Tang, H.; Li, Y.; Lahasky, S. H.; Sheiko, S. S.; Zhang, D. Core—Shell Molecular Bottlebrushes with Helical Polypeptide Backbone: Synthesis, Characterization, and Solution Conformations. *Macromolecules* **2011**, *44*, 1491-1499.
- 12. Li, Y.; Themistou, E.; Zou, J.; Das, B. P.; Tsianou, M.; Cheng, C. Facile Synthesis and Visualization of Janus Double-Brush Copolymers. *ACS Macro Lett.* **2012**, *1*, 52–56.
- 13. Liu, J.; Burts, A. O.; Li, Y.; Zhukhovitskiy, A. V.; Ottaviani, M. F.; Turro, N. J.; Johnson, J. A. "Brush-First" Method for the Parallel Synthesis of Photocleavable, Nitroxide-Labeled Poly(ethylene glycol) Star Polymers. *J. Am. Chem. Soc.* **2012**, *134*, 16337–16344.
- 14. Fenyves, R.; Schmutz, M.; Horner, I. J.; Bright, F. V.; Rzayev, J. Aqueous Self-Assembly of Giant Bottlebrush Block Copolymer Surfactants as Shape-Tunable Building Blocks. *J. Am. Chem. Soc.* **2014**, *136*, 7762-7770.
- 15. Luo, H.; Szymusiak, M.; Garcia, E. A.; Lock, L. L.; Cui, H.; Liu, Y.; Herrera-Alonso, M. Solute-Triggered Morphological Transitions of an Amphiphilic Heterografted Brush Copolymer as a Single-Molecule Drug Carrier. *Macromolecules* **2017**, *50*, 2201-2206.
- 16. Liu, W.; Liu, Y.; Zeng, G.; Liu, R.; Huang, Y. Coil-to-Rod Conformational Transition and Single Chain Structure of Graft Copolymer by Tuning the Graft Density. *Polymer* **2012**, *53*, 1005-1014.
- 17. Sheiko, S. S.; Sumerlin, B. S.; Matyjaszewski, K. Cylindrical Molecular Brushes: Synthesis, Characterization, and Properties. *Prog. Polym. Sci.* **2008**, *33*, 759-785.

- 18. Lee, H.-I.; Pietrasik, J.; Sheiko, S. S.; Matyjaszewski, K. Stimuli-Responsive Molecular Brushes. *Prog. Polym. Sci.* **2010**, *35*, 24-44.
- 19. Sheiko, S.; Möller, M. Visualization of Macromolecules A First Step to Manipulation and Controlled Response. *Chem. Rev.* **2001**, *101*, 4099-4122.
- 20. Yuan, J. Y.; Müller, A. H. E.; Matyjaszewski, K.; Sheiko, S. S. Molecular Brushes. In *Polymer Science: A Comprehensive Reference*; Elsevier: **2012**; Vol. 6, pp 199–264.
- 21. Sheiko, S. S.; Prokhorova, S. A.; Beers, K. L.; Matyjaszewski, K.; Potemkin, I. I.; Khokhlov, A. R.; Möller, M. Single Molecule Rod–Globule Phase Transition for Brush Molecules at a Flat Interface. *Macromolecules* **2001**, *34*, 8354-8360.
- 22. Stephan, T.; Muth, S.; Schmidt, M. Shape Changes of Statistical Copolymacromonomers: From Wormlike Cylinders to Horseshoe- and Meanderlike Structures. *Macromolecules* **2002**, *35*, 9857-9860.
- 23. Sun, F.; Sheiko, S. S.; Moeller, M.; Beers, K.; Matyjaszewski, K. Conformational Switching of Molecular Brushes in Response to the Energy of Interaction with the Substrate. *J. Phys. Chem. A* **2004**, *108*, 9682–9686.
- 24. Gallyamov, M. O.; Tartsch, B.; Khokhlov, A. R.; Sheiko, S. S.; Boerner, H. G.; Matyjaszewski, K.; Möller, M. Reversible Collapse of Brushlike Macromolecules in Ethanol and Water Vapours as Revealed by Real-Time Scanning Force Microscopy. *Chem. Eur. J.* **2004**, *10*, 4599–4605.
- 25. Li, C.; Gunari, N.; Fischer, K.; Janshoff, A.; Schmidt, M. New Perspectives for the Design of Molecular Actuators: Thermally Induced Collapse of Single Macromolecules from Cylindrical Brushes to Spheres. *Angew. Chem. Int. Ed.* **2004**, *43*, 1101-1104.
- 26. Lee, H.-I.; Pietrasik, J.; Matyjaszewski, K. Phototunable Temperature-Responsive Molecular Brushes Prepared by ATRP. *Macromolecules* **2006**, *39*, 3914–3920.
- 27. Yamamoto, S.-i.; Pietrasik, J.; Matyjaszewski, K. ATRP Synthesis of Thermally Responsive Molecular Brushes from Oligo(ethylene oxide) Methacrylates. *Macromolecules* **2007**, *40*, 9348-9353.
- 28. Xu, Y.; Bolisetty, S.; Drechsler, M.; Fang, B.; Yuan, J.; Ballauff, M.; Müller, A. X. E. pH and Salt Responsive Poly(*N*,*N*-dimethylaminoethyl methacrylate) Cylindrical Brushes and their Quaternized Derivatives. *Polymer* **2008**, *49*, 3957–3964.
- 29. Xu, Y.; Bolisetty, S.; Drechsler, M.; Fang, B.; Yuan, J.; Harnau, L.; Ballauff, M.; Müller, A. X. E. Manipulating Cylindrical Polyelectrolyte Brushes on the Nanoscale by Counterions: Collapse Transition to Helical Structures. *Soft Matter* **2009**, *5*, 379–384.
- 30. Lee, H.-I.; Boyce, J.R.; Nese, A.; Sheiko, S. S.; Matyjaszewski, K. pH-Induced Conformational Changes of Loosely Grafted Molecular Brushes Containing Poly(acrylic acid) Side Chains. *Polymer* **2008**, *49*, 5490-5496.
- 31. Xu, Y.; Bolisetty, S.; Ballauff, M.; Müller, A. H. E. Switching the Morphologies of Cylindrical Polycation Brushes by Ionic and Supramolecular Inclusion Complexes. *J. Am. Chem. Soc.* **2009**, *131*, 1640–1641.
- 32. Gunari, N.; Cong, Y.; Zhang, B.; Fischer, K.; Janshoff, A.; Schmidt, M. Surfactant-Induced Helix Formation of Cylindrical Brush Polymers with Poly(L-lysine) Side Chains. *Macromol. Rapid Commun.* **2008**, *29*, 821-825.
- 33. Weller, D.; McDaniel, J. R.; Fischer, K.; Chilkoti, A.; Schmidt, M. Cylindrical Polymer Brushes with Elastin-Like Polypeptide Side Chains. *Macromolecules* **2013**, *46*, 4966-4971.
- 34. Yao, J.; Chen, Y.; Zhang, J.; Bunyard, C.; Tang, C. Cationic Salt-Responsive Bottle-Brush Polymers. *Macromol. Rapid Commun.* **2013**, *34*, 645-651.

- 35. Kutnyanszky, E.; Hempenius, M. A.; Vancso, G. J. Polymer Bottlebrushes with a Redox Responsive Backbone Feel the Heat: Synthesis and Characterization of Dual Responsive Poly(ferrocenylsilane)s with PNIPAM Side Chains. *Polym. Chem.* **2014**, *5*, 771-783.
- 36. Henn, D. M.; Fu, W. X.; Mei, S.; Li, C. Y.; Zhao, B. Temperature-Induced Shape Changing of Thermosensitive Binary Heterografted Linear Molecular Brushes between Extended Worm-Like and Stable Globular Conformations. *Macromolecules* **2017**, *50*, 1645-1656.
- 37. Henn, D. M.; Lau, C. M.; Li, C. Y.; Zhao, B. Light-Triggered Unfolding of Single Linear Molecular Bottlebrushes from Compact Globular to Wormlike Nano-Objects in Water. *Polym. Chem.* **2017**, *8*, 2702-2712.
- 38. Gao, H. F.; Matyjaszewski, K. Synthesis of Molecular Brushes by "Grafting onto" Method: Combination of ATRP and Click Reactions. *J. Am. Chem. Soc.* **2007**, *129*, 6633-6639.
- 39. Yan, Y.; Shi, Y.; Zhu, W.; Chen, Y. Highly Efficient Synthesis of Cylindrical Polymer Brushes with Various Side Chains via Click Grafting-Onto Approach. *Polymer* **2013**, *54*, 5634-5642.
- 40. Iha, R. K.; Wooley, K. L.; Nyström, A. M.; Burke, D. J.; Kade, M. J.; Hawker, C. J. Applications of Orthogonal "Click" Chemistries in the Synthesis of Functional Soft Materials. *Chem. Rev.* **2009**, *109*, 5260-5685.
- 41. Jiang, X. G.; Zhao, B. End Group Effect on the Thermosensitive Properties of Well-Defined Water-Soluble Polystyrenics with Short Pendant Oligo(ethylene glycol) Groups Synthesized by Nitroxide-Mediated Radical Polymerization. *J. Polym. Sci. Part A: Polym. Chem.* **2007**, 45, 3707-3721.
- 42. Wright, R. A. E.; Henn, D. M.; Zhao, B. Thermally Reversible Physically Crosslinked Hybrid Network Hydrogels Formed by Thermosensitive Hairy NPs. *J. Phys. Chem. B* **2016**, *120*, 8036-8045.
- 43. Guo, A.; Liu, G.; Tao, J. Star Polymers and Nanospheres from Cross-Linkable Diblock Copolymers. *Macromolecules* **1996**, *29*, 2487-2493.
- 44. Tao, J.; Guo, A.; Liu, G. Adsorption of Polystyrene-*block*-poly(2-cinnamoylethyl methacrylate) by Silica from Block-Selective Solvent Mixtures. *Macromolecules* **1996**, *29*, 1618-1624.
- 45. Hua, F. J.; Jiang, X. G.; Li, D. J.; Zhao, B. Well-Defined Thermosensitive, Water-Soluble Polyacrylates and Polystyrenics with Short Pendant Oligo(ethylene glycol) Groups Synthesized by Nitroxide-Mediated Radical Polymerization. *J. Polym. Sci. Part A: Polym. Chem.* **2006**, *44*, 2454-2467.
- 46. Jin, N. X.; Woodcock, J. W., Xue, C. M.; O'Lenick, T. G.; Jiang, X. G.; Jin, S.; Dadmun, M. D.; Zhao, B. Tuning of Thermo-Triggered Gel-to-Sol Transition of Aqueous Solution of Multi-Responsive Diblock Copolymer Poly(methoxytri(ethylene glycol) acrylate-co-acrylic acid)-b-poly(ethoxydi(ethylene glycol) acrylate). *Macromolecules* **2011**, *44*, 3556-3566.
- 47. Jin, N. X.; Zhang, H.; Jin, S.; Dadmun, M. D.; Zhao, B. Tuning of Thermally Induced Solto-Gel Transitions of Moderately Concentrated Aqueous Solutions of Doubly Thermosensitive Hydrophilic Diblock Copolymers Poly(methoxytri(ethylene glycol) acrylate)-b-poly(ethoxydi(ethylene glycol) acrylate-co-acrylic acid). *J. Phys. Chem. B.* **2012**, *116*, 3125-3137.
- 48. Henn, D. M.; Wright, R. A. E.; Woodcock, J. W.; Hu, B.; Zhao, B. Tertiary Amine-Containing Thermo- and pH-Sensitive Hydrophilic ABA Triblock Copolymers: Effect of Different Tertiary Amines on Thermally Induced Sol-Gel Transitions. *Langmuir* **2014**, *30*, 2541–2550.

## **Table of Contents Graphic**

